

## Radiation Absorbed Doses from Iron-52, Iron-55, and Iron-59 Used to Study Ferrokinetics

J. S. Robertson, R. R. Price, T. F. Budinger, V. F. Fairbanks, and M. Pollycove

*Task Group of the Medical Internal Radiation Dose Committee, Society of Nuclear Medicine*

**J Nucl Med 24: 339-348, 1983**

### RADIOPHARMACEUTICAL

Radiopharmaceuticals labeled with Fe-52, Fe-55, or Fe-59 are used in studies of iron metabolism. Accelerator-produced Fe-52 and accelerator- or reactor-produced Fe-55 and Fe-59 are available in acid solutions as the chloride, citrate, or sulfate. Fe-59 has also been used as ferric or ferrous ammonium citrate.

For calculations of radiation absorbed dose, 100% radionuclidic and radiochemical purity of each radiopharmaceutical is assumed. Actually, the reactor-produced isotopes Fe-59 and Fe-55 are slightly contaminated with each other, and Fe-52 may be contaminated with Fe-55. Also, Fe-52 decays to radioactive Mn-52m and Mn-52, some of which are injected with the Fe-52. Because of the low yield of Mn-52, its contribution to the absorbed dose is negligible. The absorbed dose from the Mn-52m produced after injection is included in the dose estimate for Fe-52, but the dose from Mn-52m produced before injection is considered separately.

### NUCLEAR DATA

The nuclear data for the radioisotopes of iron and manganese considered in this report are given in Table 1.

### DOSE CALCULATION METHOD

The calculations reported in this article are based on the method described in MIRD Pamphlet No. 1, Revised (1), with:

Received Nov. 29, 1982; revision accepted Nov. 29, 1982.

For reprints contact: James S. Robertson, MD, PhD, Diagnostic Nuclear Medicine, Hilton C-66, Mayo Clinic, Rochester, MN, 55905.

$$\bar{D}(r_k) = \sum_h \bar{A}_h(0, \infty) S(r_k \leftarrow r_h) \quad (1)$$

where  $\bar{D}(r_k)$  is the mean absorbed dose in any target region  $r_k$  from any source region  $r_h$ .  $\bar{A}_h(0, \infty) = \int_0^\infty A_h dt$  is the cumulated activity in the source region; and  $S(r_k \leftarrow r_h)$  is the absorbed dose in  $r_k$  per unit cumulated activity in  $r_h$ .

It is customary to express  $\bar{A}$  relative to the administered activity,  $A_0$ . The quotient  $\bar{A}/A_0$  has the dimension of time, and is defined as the residence time,  $\tau$ , (1,2). Multiplication of  $\tau$  by  $S$  yields the absorbed dose per unit administered activity.

The sources of the  $S$  and  $\tau$  values needed for the calculations are discussed in the following sections.

### S VALUES

Most of the required  $S$  values are from MIRD Pamphlet No. 11 (3). Those for the heart are from Coffey and Watson (4). In both these references, the  $S$  values are calculated for the standard phantom described in MIRD Pamphlet No. 5, Revised (5).

However, in patients with hematological diseases, and to a lesser extent even in normal subjects, the mass, shape, and red blood cell (RBC) content of the spleen can vary markedly. In order to take the variation with mass into account, a set of  $S(\text{spleen} \leftarrow \text{spleen})$  values was calculated for each of the nuclides under consideration and for spleen mass ( $m$ ) of 100 to 4000 g. Analysis of the data tabulated in MIRD Pamphlets Nos. 3 (6) and 8 (7) shows that for a given shape of the target organ the absorbed fractions for penetrating radiations of a given energy are proportional to the cube root of the mass ( $m^{1/3}$ ). Therefore, the resulting penetrating radiation component of the  $S$  values is proportional to  $m^{-2/3}$ .

**TABLE 1. NUCLEAR DATA**

Radionuclide	Fe-52			Mn-52m			Fe-55			Fe-59		
Physical half-life	8.275 h			21.1 min			1000.4 d			44.5 d		
Mode of decay	E.C., $\beta^+$ to Mn-52m			E.C., $\beta^+$ , IT 1.9% to Mn-52			E.C.			$\beta^-$		
$\Sigma\Delta_i$ for nonpenetrating radiation	0.4267			2.405			0.0123			0.2511		
Principal photons:	$E_i^*$	$n_i^\ddagger$	$\Delta_i^\dagger$	$E_i$	$n_i$	$\Delta_i$	$E_i$	$n_i$	$\Delta_i$	$E_i$	$n_i$	$\Delta_i$
	0.169	0.993	0.357	1.434	0.980	2.993	1.099	0.555	1.299	1.292	0.441	1.214
	0.511	1.156	1.258	0.511	1.931	2.101						

\*  $E_i$  - energy (MeV).  
 $\dagger\Delta_i$  - mean energy emitted per unit cumulated activity. (g-rad/ $\mu$ Ci-h)  
 $\ddagger n_i$  - mean number of particles or photons per transformation.  
 Nonpenetrating radiation includes  $\beta$ 's, electrons, and photons with  $E_i < 10$  keV.  
 The half-life data cited are abstracted from Refs. (41) and (42). Slightly different values for Mn-52m and Fe-59 appear in Ref. (43).  
 The decay-scheme data are from Ref. (43). Additional data and primary references can be found in Ref. (44).

Based on this relationship, the spleen S values were calculated by using Equation (2):

$$S(m) = S_p(173.6) \times \left(\frac{173.6}{m}\right)^{2/3} + S_{np}(173.6) \times \left(\frac{173.6}{m}\right), \quad (2)$$

- where m is spleen mass in grams,
- S(m) is S value for spleen of mass m,
- p is penetrating radiation,
- np is nonpenetrating radiation,
- 173.6 is spleen mass in standard phantom (5)

The results are presented in Table 2. The  $S_p(173.6)$  and  $S_{np}(173.6)$  values for Mn-52m, Fe-55, and Fe-59 were obtained from ORNL-5000 (8), except that for Fe-55 all of the radiation was considered to be nonpenetrating because the penetrating fraction consists only of x-rays having energies less than 10 keV. The  $S(173.6)$  values for Fe-52 were derived from the  $S(\text{spleen} \leftarrow \text{spleen})$  value in MIRD-11 (3) ( $3.1 \times 10^{-3}$  rad/ $\mu$ Ci-h) and the  $\Delta$  values given in Table 1.

IRON KINETICS

**General.** There is an extensive literature on iron ki-

**TABLE 2. S(SPLEEN ← SPLEEN)**  
(rad/ $\mu$ Ci-h)

Spleen mass (grams)	Fe-52	Mn-52m	Fe-55	Fe-59
100	$52 \times 10^{-4}$	$26 \times 10^{-3}$	$12 \times 10^{-5}$	$39 \times 10^{-4}$
173.6*	$31 \times 10^{-4}$	$15 \times 10^{-3}$	$7.0 \times 10^{-5}$	$24 \times 10^{-4}$
200	$27 \times 10^{-4}$	$14 \times 10^{-3}$	$6.1 \times 10^{-5}$	$21 \times 10^{-4}$
300	$19 \times 10^{-4}$	$9.2 \times 10^{-3}$	$4.0 \times 10^{-5}$	$15 \times 10^{-4}$
400	$14 \times 10^{-4}$	$7.0 \times 10^{-3}$	$3.0 \times 10^{-5}$	$12 \times 10^{-4}$
500	$12 \times 10^{-4}$	$5.7 \times 10^{-3}$	$2.4 \times 10^{-5}$	$9.8 \times 10^{-4}$
600	$10 \times 10^{-4}$	$4.8 \times 10^{-3}$	$2.0 \times 10^{-5}$	$8.5 \times 10^{-4}$
700	$8.6 \times 10^{-4}$	$4.1 \times 10^{-3}$	$1.7 \times 10^{-5}$	$7.5 \times 10^{-4}$
800	$7.6 \times 10^{-4}$	$3.7 \times 10^{-3}$	$1.5 \times 10^{-5}$	$6.7 \times 10^{-4}$
900	$6.9 \times 10^{-4}$	$3.3 \times 10^{-3}$	$1.4 \times 10^{-5}$	$6.1 \times 10^{-4}$
1000	$6.3 \times 10^{-4}$	$3.0 \times 10^{-3}$	$1.2 \times 10^{-5}$	$5.6 \times 10^{-4}$
2000	$3.4 \times 10^{-4}$	$1.6 \times 10^{-3}$	$0.61 \times 10^{-5}$	$3.2 \times 10^{-4}$
3000	$2.4 \times 10^{-4}$	$1.1 \times 10^{-3}$	$0.41 \times 10^{-5}$	$2.3 \times 10^{-4}$
4000	$1.9 \times 10^{-4}$	$0.84 \times 10^{-3}$	$0.30 \times 10^{-5}$	$1.9 \times 10^{-4}$

\* MIRD-11 (3) phantom value.

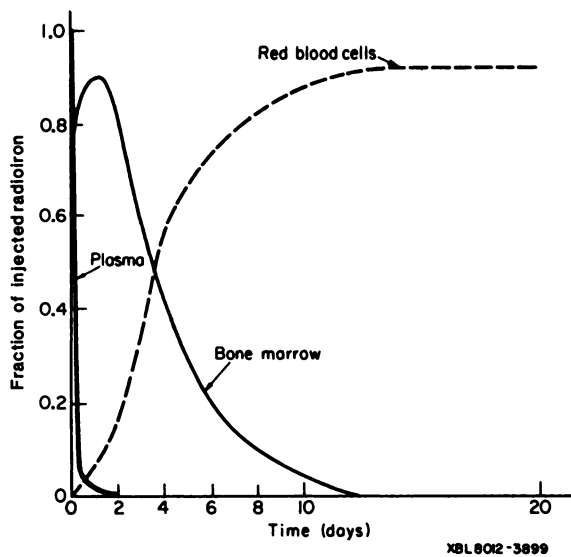


FIG. 1. Fraction of injected radioiron in blood plasma, bone marrow, and RBCs of normal subjects as a function of time. (Redrawn from Ref. 29.)

netics in normal subjects and in various disease states (9-17). Reports cited by Fairbanks et al. (18) indicate that the normal 70-kg man has a total-body iron content of about 3.7 g, of which 67% is in hemoglobin, 27% is in storage as ferritin and hemosiderin, and the remaining 6% is in other compartments. In females, there is less storage iron and less total-body iron than in males. There is a plasma-iron turnover rate of about 35 mg of iron per day, largely because of red-cell destruction and iron reutilization. About 20 mg/day is used in RBC production.

**Radioiron.** Normally, following slow intravenous injection, or if mixed with plasma before injection, radioactive iron injected as any of the agents in use is bound to transferrin rapidly. In this form most of the administered tracer is transported from the plasma to the bone marrow, where it is used in hemoglobin synthesis. Some iron is exchanged between plasma and the extravascular-extracellular fluid. Plasma iron is also exchanged with rapidly equilibrating tissue iron pools.

In normal subjects, the transferrin-bound radioiron

concentration in the plasma decreases with a half-time of 1 to 2 hr as radioiron accumulates in the bone marrow, and within 24 hr 70% to 90% of the administered activity is concentrated in the red marrow (see Fig. 1). There the tracer is incorporated into RBCs, which are released into the circulation. Radioiron remains in the marrow for 3 to 5 days. Fe-59 or Fe-55 activity in the circulation reaches 80% or more of the administered activity (corrected for decay) within 10 to 15 days. The short half-life of Fe-52 (8.2 h), combined with the 3- to 5-day residence in the red marrow, prevent any appreciable amount of this activity from reaching the circulation (19). After 10-15 days about 5% of the administered Fe-59 or Fe-55 is found in the liver and 2% to 7% is found in the spleen, primarily as activity in circulating RBCs. Approximately 5% of the administered activity is assumed to be uniformly distributed extravascularly throughout the body. The radioactivity incorporated into a RBC remains in the cell for its lifetime, which is about  $120 \pm 6$  days (20) with a range of 100 to 135 days. Upon the destruction of the RBC, its iron is released and the utilization cycle is repeated.

Total-body radioactivity measurements (21-23) indicate that normally there is an iron loss at a rate of 0.01% to 0.05% of the body iron per day (0.4 to 2 mg/day). This loss is balanced by the dietary iron intake. For this radiation dose estimate, the excretion of radioiron is neglected.

#### BIOLOGICAL DATA AND DATA PROCESSING

**Methods.** The  $\bar{A}$  and  $\tau$  values are derived from data on the kinetics of distribution of radioiron. These data include regional external counts and determinations of the activity concentrations in the plasma and in whole blood, in samples drawn at selected times. It is necessary to combine these data in a way that is consistent with known iron kinetics and yields the  $\tau$  values needed for calculations of absorbed dose. The methods used in this procedure follow those described in MIRD-12 (2). Figure 2 is an information flow diagram of this process. First, the data are used to determine the compartment

#### CALCULATION OF MEAN ABSORBED DOSE FROM RADIOIRON KINETIC DATA

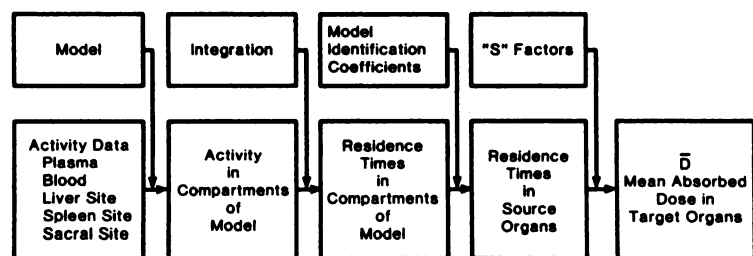
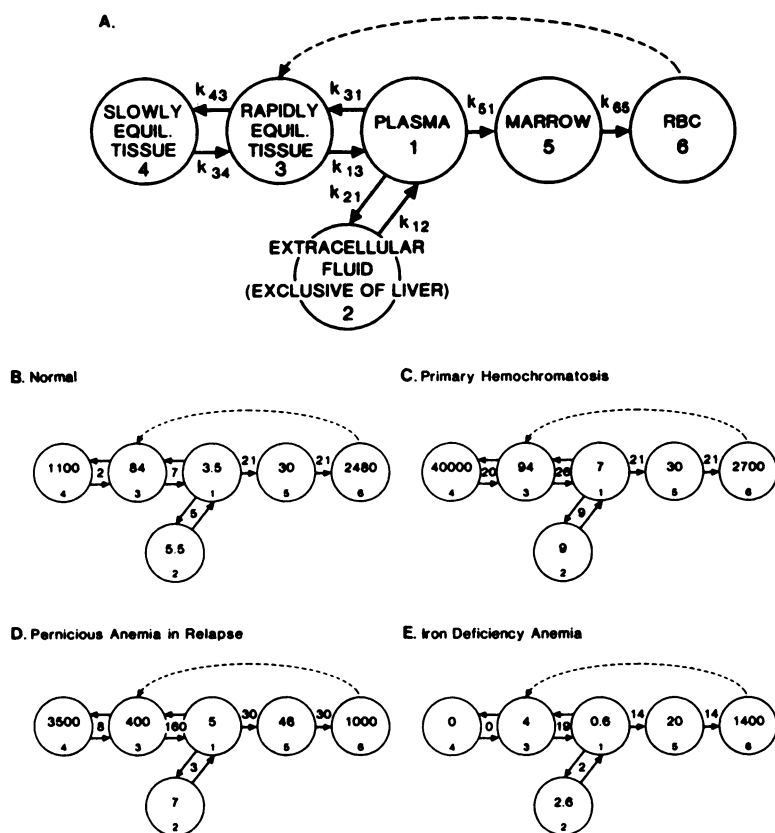


FIG. 2. Diagram of information flow in calculation of radiation absorbed dose from kinetic data.



**FIG. 3(A).** Diagram of model used with SAAM-25 program for calculating radioiron kinetic parameters (25-27). Arrows indicate rate constants,  $k$ , for intercompartmental transfer. Notation  $k_{ij}$  means fractional rate of transfer into  $i^{th}$  compartment from  $j^{th}$  compartment. Dashed line between compartments 3 and 6 indicates delayed feedback due to 120-day life of circulating RBCs. Compartment 2 includes 2 mg as rapidly exchanging iron in non-heme iron enzymes (14).

**FIG. 3(B), (C), (D), and (E).** Numerical values for quantities of iron (mg) in each compartment, and iron transfer rates (mg/day) between compartments for (B) normal, (C) primary hemochromatosis, (D) pernicious anemia in relapse, and (E) iron-deficiency anemia. When there are two arrows shown between compartments, transfer rates are assumed to be equal in the two directions. Values for rate constants  $k_{ij}$  in Fig. 3(A) are obtained from rates and compartment sizes by dividing each rate by amount in originating compartment. For example, in normal  $k_{43} = 2/84$ , but  $k_{34} = 2/1100$ . In calculation of  $k_{13}$ , we assume that additional transfer rate from rapid storage to plasma equals that from plasma to red marrow, as required for a steady-state model.

sizes and transfer rate constants that give a best fit to the data according to a mathematical model of iron kinetics. Integration of the equations that describe the kinetics in this model then yields values of  $\bar{A}$  and  $\tau$  for the compartments of the model. In general, however, these compartments do not correspond to anatomically defined organs. The conversion from a compartmental system, as represented in the model, to an anatomical system is achieved through the use of model identification coefficients. These are defined as the fractions of the substance in a model compartment that are assigned to specific organs (2). These values are used to convert the  $\tau$ 's for the compartmental system to  $\tau$ 's for the source organs. Finally, multiplication by  $S$  yields the absorbed dose per unit administered activity.

**Human data.** The data for radioiron distribution in human tissue, on which the absorbed radiation dose

calculations in the report are based, were obtained from the literature (11,14,16,18) and from other clinical studies (personal communication from R. R. Price, M. Pollycove, H. S. Winchell). Most of the data are from studies in which Fe-59 citrate was used. An RBC lifespan of 120 days was assumed for all calculations in this report.

**Modeling.** The NIH Simulation Analysis and Modeling computer program (SAAM-25) (24) was used with the model shown in Fig. 3A (25-27) to provide kinetic parameters and the cumulated activities required for estimates of radiation absorbed doses to the target organs. In the model used, the liver and spleen counts obtained with external probe systems are assumed to originate from compartments 3, 4, 5, and 6. Although compartment 5, the marrow, is not part of the liver and spleen, it is included because activity in this compartment

**TABLE 3. TRANSFER RATE CONSTANTS (FRACTION/DAY)**

	$k_{12}$	$k_{21}$	$k_{13}$	$k_{31}$	$k_{34}$	$k_{43}$	$k_{51}$	$k_{65}$
Normal	0.91	1.4	0.33	2.0	0.0018	0.024	6.0	0.70
Primary hemochromatosis	1.0	1.3	0.50	3.7	0.00050	0.21	3.0	0.70
Pernicious anemia	0.43	0.60	0.475	32	0.0023	0.020	6.0	0.65
Iron-deficiency anemia	0.77	3.3	8.25	32	0.0	0.0	23	0.70
Polycythemia vera	0.91	1.4	0.58	2.0	0.0018	0.024	12.0	0.70

**TABLE 4. RESIDENCE TIME ( $\tau$ ) BY COMPARTMENTS (HOURS)**

	1(plasma)	2(ECF)	3(rapid)	4(slow)	5(marrow)	6(RBC)
<u>Fe-52, Mn-52m</u>						
Normal	2.2	1.1	1.9	$2.3 \times 10^{-2}$	6.7	0
Primary hemochromatosis	2.7	1.2	3.7	$39 \times 10^{-2}$	4.0	0
Pernicious anemia	0.71	0.17	8.9	$8.9 \times 10^{-2}$	2.1	0
Iron-deficiency anemia	0.73	0.84	2.2	0	8.2	0
Polycythemia vera	1.4	0.70	1.3	$1.6 \times 10^{-2}$	8.5	0
<u>Fe-55</u>						
Normal	22	23	$2.7 \times 10^2$	$6.1 \times 10^3$	$1.3 \times 10^2$	$28 \times 10^3$
Primary hemochromatosis	19	18	$1.3 \times 10^2$	$28 \times 10^3$	$0.58 \times 10^2$	$6.8 \times 10^3$
Pernicious anemia	75	29	$15 \times 10^2$	$14 \times 10^3$	$1.9 \times 10^2$	$19 \times 10^3$
Iron-deficiency anemia	21	16	$0.31 \times 10^2$	0	$1.3 \times 10^2$	$34 \times 10^3$
Polycythemia vera	14	12	$1.3 \times 10^2$	$3.2 \times 10^3$	$1.3 \times 10^2$	$31 \times 10^3$
<u>Fe-59</u>						
Normal	6.9	7.2	36	$0.5 \times 10^2$	39	$14 \times 10^2$
Primary hemochromatosis	9.0	8.3	37	$4.8 \times 10^2$	27	$9.8 \times 10^2$
Pernicious anemia	13	4.6	220	$2.5 \times 10^2$	31	$10 \times 10^2$
Iron-deficiency anemia	7.0	5.3	7.5	0	41	$15 \times 10^2$
Polycythemia vera	4.5	3.7	15	$0.3 \times 10^2$	40	$15 \times 10^2$

contributes to the external counts obtained in the liver and spleen areas. Later, however, when the  $\tau$ 's in the compartments are redistributed to yield the  $\tau$ 's in the body organs, the marrow activity is separated from that in the liver and spleen.

**Transfer rate constants.** The normal transfer rate constants shown in Table 3 were derived in part by fitting the model to the data for each subject. Values within the ranges of the fits were selected for conformity with established normal values of compartment sizes in the literature on iron kinetics. With the assumption that the total iron in the body is 3.7 g (18), the transfer rate constants were used to calculate the sizes of the compartments, in mg of iron, and the intercompartmental transfer rates, in mg of iron per day. The values for the idealized normal subject are shown in Fig. 3b.

The rate constants for the disease states were obtained through the reverse procedure. That is, literature values for the compartment sizes and transfer rates, drawn principally from Refs. 14 and 16, were used to calculate the transfer rate constants. The values used are indicated in Figs. 3C, 3D, and 3E for primary hemochromatosis, pernicious anemia in relapse, and iron-deficiency anemia, respectively. The model used for polycythemia vera (not illustrated) differs from the normal only in having a doubled rate of transfer through the marrow into the RBC compartment, with a consequent doubling of the marrow and RBC compartments and of  $k_{51}$ . This represents only one of several possible states in this complex disease.

**Cumulated activity and residence times in model compartments.** The kinetic parameters established above

**TABLE 5. MODEL IDENTIFICATION COEFFICIENTS (NORMAL) (FRACTION OF COMPARTMENT IN ORGAN)**

Compartment	Organ					
	Liver	Spleen	Red marrow	Heart	RBC*	Residual
1. Plasma	0.08	0.01	0.04	0.08	—	0.79
2. ECF	0.03	0.01	0.03	—	—	0.93
3. Rapid storage	—	—	1.0	—	—	—
4. Slow storage	0.33	0.15	0.30	—	—	0.22
5. Red marrow	—	—	1.0	—	—	—
6. RBC	0.05	0.05	0.04	0.08	0.78	—

\* RBC outside of named organs.

were used with the physical half-lives to generate corresponding activity-time curves in the compartments of the model for Fe-52, Fe-55, and Fe-59. The effect of the recycling because of the finite RBC lifetime was approximated by transferring all of the RBC activity to the rapid-storage compartment at 120-day intervals. The SAAM-25 program was then used to carry out a numerical integration of the activity-time curves to determine the cumulated activities per unit administered activity, or residence times. The integration limits for Fe-59 and Fe-52 were chosen to be approximately ten times the respective physical half-lives. For Fe-55 a numerical integration was carried out for a period of 400 days, after which time the contents of the compartments were assumed to diminish through physical decay only. The residence times for radioiron in the compartments of the model are given in Table 4.

**Model identification coefficients (Table 5).** These were determined by fitting the model to the original Fe-59 external counting data. For the normal, it is assumed that 8% of the blood is in the heart (28), and 5% of the circulating RBCs are in the liver (29), but 8% of the plasma is assigned to the liver to allow for the known low hematocrit in this organ. The fraction of RBCs outside of the named organs is listed separately. For compartments 1-5, the fractions outside of the named organs are tabulated as "residual".

The spleen RBC content presents a special problem. Although autopsy studies indicate low blood volumes in the spleen, in-vivo studies show that a large mass of red blood cells may be sequestered in the spleen (30). The fraction of the red-cell mass found in the normal spleen by various methods varies between 0.01 and 0.1 (31-33). For the tabulated dose estimates, 0.05 of the RBCs and 0.01 of the plasma are assumed to be in the spleen. Estimates for spleen self-irradiation for other cases can be

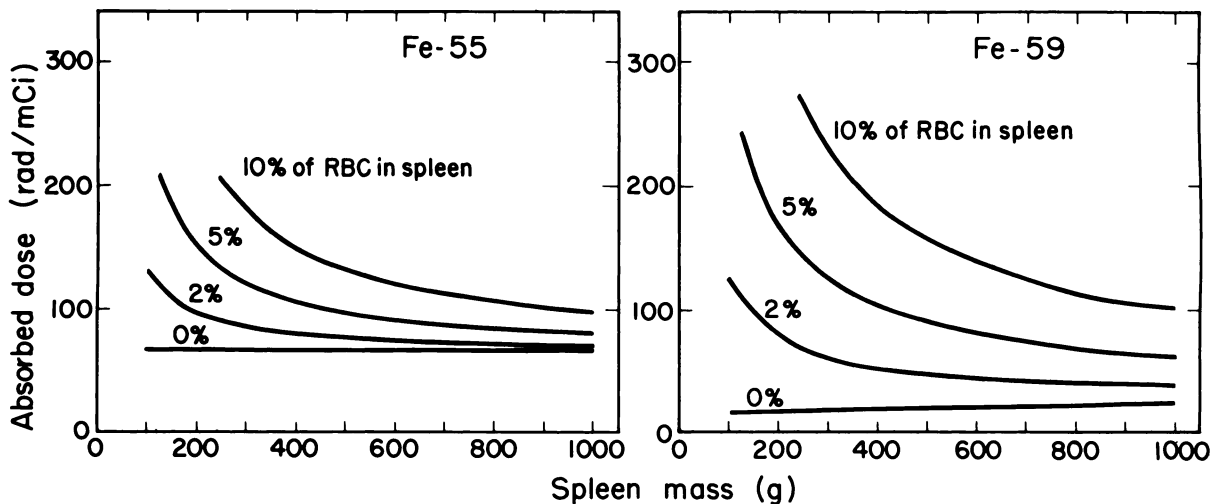
made from Fig. 4. With splenic enlargement, 0.3 or more of the total red-cell mass can be found in the spleen. The splenic RBC pool is increased in polycythemia vera (34).

**Residence times in source organs.** The  $\tau$ 's determined for the compartments of the model were redistributed through the use of the model identification coefficients to give the  $\tau$ 's for the marrow, RBC's, liver, spleen, heart, and residual. The results are shown in Table 6. The  $\tau$ 's tabulated for "RBC" in Table 6 represent the remaining fraction of RBCs outside of the named source organ. (For total RBC  $\tau$ 's, see Table 4.)

#### MANGANESE-52m

This nuclide has a relatively short half-life (21.1 min) and reaches transient equilibrium with Fe-52 in less than 2 hr. Therefore, the value of  $\tau$  for Mn-52m produced by decay of Fe-52 after injection is taken to be equal to the  $\tau$  of Fe-52. The available information (35-37) indicates that the Mn-52m decays at or near the site of its production, so the distribution of the Mn-52m formed by decay after injection is assumed to be identical with that of Fe-52.

Manganese-52m injected with the Fe-52 will differ in distribution from that of the Mn-52m produced after injection. Cotzias (38) has reviewed the metabolism of manganese. Atkins et al. (39) have studied the distribution kinetics of Mn-54 in mice, rats and dogs, and of Mn-52m in dogs. Halpern et al. (40) have studied the distribution of Mn-54 in rats. However, no quantitative data for the distribution of Mn-52m in human beings are available. These animal data suggest that the Mn-52m injected with Fe-52 may contribute substantially to the absorbed doses for spleen, liver, pancreas, and kidneys.



XBL8111-4358

FIG. 4. Self-irradiation doses per unit administered activity for 0, 2, 5 and 10% of total RBC activity in spleen, as functions of spleen mass, assuming total RBC mass of 2400 g (30).

**TABLE 6. RESIDENCE TIME ( $\tau$ ) IN SOURCE ORGANS (HOURS)**

	Liver	Spleen	Red marrow	Heart	RBC*	Residual
<u>Fe-52, Mn-52m</u>						
Normal	$2.2 \times 10^{-1}$	$3.7 \times 10^{-2}$	8.7	$18 \times 10^{-2}$	0	2.8
PH	$3.8 \times 10^{-1}$	$10 \times 10^{-2}$	8.0	$22 \times 10^{-2}$	0	3.3
PAR	$0.90 \times 10^{-1}$	$2.2 \times 10^{-2}$	11	$5.5 \times 10^{-2}$	0	0.74
IDA	$0.83 \times 10^{-1}$	$1.6 \times 10^{-2}$	10	$5.8 \times 10^{-2}$	0	1.4
PV	$1.4 \times 10^{-1}$	$2.2 \times 10^{-2}$	9.9	$12 \times 10^{-2}$	0	1.8
<u>Fe-55</u>						
Normal	$3.4 \times 10^3$	$2.3 \times 10^3$	$3.3 \times 10^3$	$2.2 \times 10^3$	$2.2 \times 10^4$	$1.4 \times 10^3$
PH	$9.5 \times 10^3$	$4.5 \times 10^3$	$8.7 \times 10^3$	$0.54 \times 10^3$	$0.53 \times 10^4$	$6.1 \times 10^3$
PAR	$5.6 \times 10^3$	$3.0 \times 10^3$	$6.6 \times 10^3$	$1.5 \times 10^3$	$1.5 \times 10^4$	$3.2 \times 10^3$
IDA	$1.7 \times 10^3$	$1.7 \times 10^3$	$1.4 \times 10^3$	$2.8 \times 10^3$	$2.7 \times 10^4$	$0.032 \times 10^3$
PV	$2.6 \times 10^3$	$2.0 \times 10^3$	$2.5 \times 10^3$	$2.5 \times 10^3$	$2.4 \times 10^4$	$0.73 \times 10^3$
<u>Fe-59</u>						
Normal	$8.7 \times 10^1$	$7.8 \times 10^1$	$15 \times 10^1$	$11 \times 10^1$	$11 \times 10^2$	$2.3 \times 10^1$
PH	$21 \times 10^1$	$12 \times 10^1$	$25 \times 10^1$	$7.9 \times 10^1$	$7.6 \times 10^2$	$12 \times 10^1$
PAR	$13 \times 10^1$	$8.8 \times 10^1$	$37 \times 10^1$	$8.3 \times 10^1$	$8.0 \times 10^2$	$6.9 \times 10^1$
IDA	$7.5 \times 10^1$	$7.4 \times 10^1$	$11 \times 10^1$	$12 \times 10^1$	$12 \times 10^2$	$1.0 \times 10^1$
PV	$8.0 \times 10^1$	$7.6 \times 10^1$	$12 \times 10^1$	$12 \times 10^1$	$11 \times 10^2$	$1.2 \times 10^1$

\* RBC outside of named organs. For total RBC see Table 4.

PH - primary hemochromatosis.

PAR - pernicious anemia in relapse.

IDA - iron-deficiency anemia.

PV - polycythemia vera.

The amount of Mn-52m injected with the Fe-52 depends upon the time elapsed between separation and injection. The Fe-52 dose estimates that follow do not include any estimate of the absorbed dose due to injected Mn-52m, but do include the absorbed dose from Mn-52m produced by the decay of Fe-52 after it has been injected.

#### RADIATION ABSORBED DOSE

In the radiation dose calculation, the source organs are those listed in Table 6. The target organs are the liver, spleen, red marrow, ovaries, testes, kidneys, heart wall, and total body. When the source is RBC or residual, and the target organs are the gonads, kidneys, and total body, the  $S(\text{target organ} \leftarrow \text{total body})$  values (3) are used. However, when the source is RBC or residual and the target organs are the named source organs, the  $S(\text{target organ} \leftarrow \text{other})$  values (3) are used in order to exclude the nonpenetrating component of the dose, since by definition RBC and residual activities lie outside of the named source organs. The mean absorbed doses per unit administered activity for each isotope of iron and for each source-target organ pair were calculated by use of Eq. 1. The results for normal subjects in units of rad/mCi are listed in Table 7.

Similarly, the mean absorbed doses per unit admin-

istered activity were calculated for each of the types of patient under consideration. The sums for each target organ are presented in Tables 8-10. All of these results were obtained using the S values for reference man (3).

In some of the diseases, there can be appreciable changes in the spleen size and in the amount of RBC sequestration in the spleen, so special calculations have been made for the self-irradiation dose to the spleen as functions of its mass and RBC content. Figure 4 presents the results obtained for the mean absorbed doses in the spleen for 0, 2, 5, and 10% of the total RBC cumulated activity in the spleen, for Fe-55 and Fe-59 and for spleen masses 100-1000 g. The curves show the dose for the indicated fraction of the total RBC cumulated activity plus the non-RBC cumulated activity.

In the calculation of these curves, the  $\tau$  values for non-RBC activity in the spleen were assumed to be proportional to the splenic mass, with the reference values being  $\tau(\text{Fe-55}) = 914$  h and  $\tau(\text{Fe-59}) = 7.6$  h, for non-RBC activity in a 173.6 g spleen. As an example of the spleen dose calculations, consider the Fe-59 dose in a 500-gram spleen containing 2% of the RBCs. The normal RBC  $\tau$  is 1400 h (Table 4), and 2% of this is 28 h. The non-RBC Fe-59  $\tau$  value is  $7.6 \times 500/173.6 = 22$  h. Thus the total  $\tau$  is 50 h. From Table 2 the Fe-59  $S(\text{spleen} \leftarrow \text{spleen})$  value for a 500-g spleen is  $9.8 \times 10^{-4}$

**TABLE 7. MEAN RADIATION ABSORBED DOSE PER UNIT ADMINISTERED ACTIVITY IN NORMAL SUBJECTS FROM RADIOIRON (rad/mCi)**

Target Organ	Source organ					Residual	Sum
	Liver	Spleen	Red marrow	Heart	RBC*		
<b>Fe-52 + Mn-52m</b>							
Liver	$480 \times 10^{-3}$	$8.8 \times 10^{-4}$	$2.0 \times 10^{-1}$	$11 \times 10^{-3}$	0	$0.70 \times 10^{-1}$	$7.7 \times 10^{-1}$
Spleen	$5.1 \times 10^{-3}$	$6600 \times 10^{-4}$	$1.8 \times 10^{-1}$	$6.2 \times 10^{-3}$	0	$0.92 \times 10^{-1}$	$9.4 \times 10^{-1}$
Red marrow	$5.5 \times 10^{-3}$	$9.2 \times 10^{-4}$	$130 \times 10^{-1}$	$4.9 \times 10^{-3}$	0	$0.84 \times 10^{-1}$	$130 \times 10^{-1}$
Ovaries	$2.8 \times 10^{-3}$	$7.0 \times 10^{-4}$	$6.5 \times 10^{-1}$	$0.52 \times 10^{-3}$	0	$2.3 \times 10^{-1}$	$8.8 \times 10^{-1}$
Testes	$0.66 \times 10^{-3}$	$0.88 \times 10^{-4}$	$0.65 \times 10^{-1}$	$0.17 \times 10^{-3}$	0	$2.2 \times 10^{-1}$	$2.9 \times 10^{-1}$
Kidneys	$18 \times 10^{-3}$	$70 \times 10^{-4}$	$0.47 \times 10^{-1}$	$4.5 \times 10^{-3}$	0	$2.2 \times 10^{-1}$	$3.0 \times 10^{-1}$
Heart wall	$14 \times 10^{-3}$	$18 \times 10^{-4}$	$2.3 \times 10^{-1}$	$740 \times 10^{-3}$	0	$2.2 \times 10^{-1}$	$12 \times 10^{-1}$
Total body	$17 \times 10^{-3}$	$29 \times 10^{-4}$	$6.6 \times 10^{-1}$	$14 \times 10^{-3}$	0	$2.0 \times 10^{-1}$	$9.0 \times 10^{-1}$
<b>Fe-55</b>							
Liver	24	<	$0.057 \times 10^{-2}$	<	0.026	$0.16 \times 10^{-2}$	24
Spleen	<	160	$0.10 \times 10^{-2}$	<	0.050	$0.32 \times 10^{-2}$	160
Red marrow	$0.04 \times 10^{-2}$	$0.03 \times 10^{-3}$	25	<	0.088	$0.55 \times 10^{-2}$	26
Ovaries	<	<	$0.057 \times 10^{-2}$	<	4.2	$26 \times 10^{-2}$	4.4
Testes	<	<	$0.0016 \times 10^{-2}$	<	3.9	$25 \times 10^{-2}$	4.2
Kidneys	$0.58 \times 10^{-2}$	$32 \times 10^{-3}$	$0.16 \times 10^{-2}$	<	3.9	$25 \times 10^{-2}$	4.2
Heart wall	<	<	<	$3.2 \times 10^1$	3.9	$24 \times 10^{-2}$	36
Total body	$60 \times 10^{-2}$	$410 \times 10^{-3}$	$59 \times 10^{-2}$	$4.0 \times 10^{-1}$	3.9	$24 \times 10^{-2}$	6.1
<b>Fe-59</b>							
Liver	30	0.69	1.2	$24 \times 10^{-1}$	$0.99 \times 10^1$	$2.1 \times 10^{-1}$	$4.4 \times 10^1$
Spleen	0.77	190	1.2	$1.4 \times 10^{-1}$	$1.3 \times 10^1$	$2.8 \times 10^{-1}$	$20 \times 10^1$
Red marrow	0.72	0.70	29	$11 \times 10^{-1}$	$1.1 \times 10^1$	$2.3 \times 10^{-1}$	$4.3 \times 10^1$
Ovaries	0.63	0.37	3.5	$2.1 \times 10^{-1}$	$1.9 \times 10^1$	$3.9 \times 10^{-1}$	$2.4 \times 10^1$
Testes	0.16	0.078	0.41	$0.47 \times 10^{-1}$	$1.9 \times 10^1$	$3.9 \times 10^{-1}$	$2.0 \times 10^1$
Kidneys	2.6	5.0	2.9	$9.9 \times 10^{-1}$	$2.0 \times 10^1$	$4.1 \times 10^{-1}$	$3.2 \times 10^1$
Heart wall	2.1	1.2	1.3	$670 \times 10^{-1}$	$1.8 \times 10^1$	$3.8 \times 10^{-1}$	$9.0 \times 10^1$
Total body	1.5	1.3	2.3	$20 \times 10^{-1}$	$1.6 \times 10^1$	$3.5 \times 10^{-1}$	$2.4 \times 10^1$

\* Dose from RBC activity outside of the named source organs.  
 < Indicates dose less than  $10^{-8}$  rad/mCi.

**TABLE 8. RADIATION ABSORBED DOSE PER UNIT ADMINISTERED ACTIVITY FOR Fe-52 + Mn-52m\* rad/mCi (mGy/MBq)**

	Normal	Primary hemochromatosis	Pernicious anemia in relapse	Iron-deficiency anemia	Polycythemia vera
Liver†	0.77 (0.21)	1.1 (0.30)	0.48 (0.13)	0.46 (0.12)	0.59 (0.16)
Spleen†	0.94 (0.25)	2.0 (0.55)	0.65 (0.18)	0.54 (0.15)	0.69 (0.19)
Red marrow	13 (3.6)	12 (3.3)	17 (4.5)	16 (4.2)	15 (4.0)
Ovaries	0.88 (0.24)	0.87 (0.23)	0.88 (0.24)	0.89 (0.24)	0.88 (0.24)
Testes	0.29 (0.078)	0.32 (0.087)	0.14 (0.038)	0.19 (0.050)	0.22 (0.059)
Kidneys	0.30 (0.080)	0.36 (0.096)	0.13 (0.035)	0.17 (0.047)	0.21 (0.058)
Heart wall	1.2 (0.33)	1.4 (0.37)	0.59 (0.16)	0.63 (0.17)	0.90 (0.24)
Total body	0.90 (0.24)	0.90 (0.24)	0.91 (0.25)	0.90 (0.24)	0.90 (0.24)

Doses in conventional units and in SI units were rounded to two significant figures from separate calculations, so some minor discrepancies in conversion between the two systems may appear.

\* Doses include the contribution from Mn-52m produced after injection of Fe-52 but do not include Mn-52m produced before injection.

† No myeloproliferative tissue in liver and spleen is assumed. Its presence increases the dose to these organs.



**TABLE 9. RADIATION ABSORBED DOSE PER UNIT ADMINISTERED ACTIVITY FOR Fe-55  
rad/mCi (mGy/MBq)**

	Normal	Primary hemochromatosis	Pernicious anemia in relapse	Iron- deficiency anemia	Polycythemia vera
Liver	24 (6.5)	66 (18)	39 (11)	12.1 (3.2)	18 (5.0)
Spleen*	160 (44)	310 (85)	210 (58)	120 (33)	140 (38)
Red marrow	26 (6.9)	67 (18)	51 (14)	12 (3.2)	19 (5.1)
Ovaries	4.4 (1.2)	2.2 (0.58)	3.4 (0.92)	5.1 (1.4)	4.7 (1.3)
Testes	4.2 (1.1)	2.0 (0.55)	3.2 (0.87)	4.8 (1.3)	4.5 (1.2)
Kidneys	4.2 (1.1)	2.1 (0.58)	3.3 (0.88)	4.9 (1.3)	4.5 (1.2)
Heart wall	36 (9.8)	9.7 (2.6)	25 (6.7)	44 (12)	40 (11)
Total body	6.1 (1.6)	6.1 (1.6)	6.1 (1.6)	6.1 (1.6)	6.1 (1.6)

\* Assuming 5% of RBC  $\tau$  in 173.6-g spleen. See Fig. 4 for spleen doses under other assumptions.

**TABLE 10. RADIATION ABSORBED DOSE PER UNIT ADMINISTERED ACTIVITY FOR Fe-59  
rad/mCi (mGy/MBq)**

	Normal	Primary hemochromatosis	Pernicious anemia in relapse	Iron- deficiency anemia	Polycythemia vera
Liver	44 (12)	83 (23)	59 (16)	40 (11)	42 (11)
Spleen*	200 (55)	300 (82)	230 (61)	190 (52)	200 (53)
Red marrow	43 (12)	62 (17)	85 (23)	36 (9.6)	38 (10)
Ovaries	24 (6.4)	23 (6.3)	25 (6.8)	23 (6.3)	24 (6.4)
Testes	20 (5.3)	16 (4.4)	16 (4.4)	20 (5.5)	20 (5.4)
Kidneys	32 (8.6)	36 (9.6)	33 (9.0)	31 (8.4)	31 (8.5)
Heart wall	90 (24)	70 (19)	71 (19)	93 (25)	92 (25)
Total body	24 (6.4)	24 (6.5)	24 (6.5)	24 (6.4)	24 (6.4)

\* Assuming 5% of RBC  $\tau$  in 173.6-g spleen. See Fig. 4 for spleen doses under other assumptions.

rad/ $\mu$ Ci. Therefore, the dose for this case is  $(50)(1000)(9.8 \times 10^{-4}) = 49$  rad/mCi. This result can also be read from the 2% curve of the Fe-59 graph in Fig. 4.

For Fe-52 + Mn-52m (not shown in Fig. 4), none of the total residence time is due to the RBC content, and there is a very weak dependence of the dose on the splenic mass.

If myeloproliferative tissue is present in the spleen (19), the self-irradiation dose from Fe-52 will be much higher.

#### SUMMARY

Biological data obtained principally with Fe-59 citrate are used with physical data to calculate radiation absorbed doses for ionic or weak chelate forms of Fe-52, Fe-55, and Fe-59, administered by intravenous injection. Doses are calculated for normal subjects, primary hemochromatosis (also called idiopathic or hereditary

hemochromatosis), pernicious anemia in relapse, iron-deficiency anemia, and polycythemia vera. The Fe-52 doses include the dose from the Mn-52m daughter generated after injection of Fe-52. Special attention has been given to the dose to the spleen, which has a relatively high concentration of RBCs and therefore of radioiron, and which varies significantly in size in both health and disease.

#### REFERENCES

1. LOEVINGER R, BERMAN M: A revised schema for calculating the absorbed dose from biologically distributed radionuclides. *MIRD Pamphlet No. 1, Revised*. New York, Society of Nuclear Medicine, March 1976
2. BERMAN M: Kinetic models for absorbed dose calculations. *MIRD Pamphlet No. 12*. New York, Society of Nuclear Medicine, Jan 1977
3. SNYDER WS, FORD MR, WARNER GG, et al: "S", Absorbed dose per unit cumulated activity for selected radionuclides and organs. *MIRD Pamphlet No. 11*. New York, Society of Nuclear Medicine, Oct 1975
4. COFFEY JL, WATSON EE: S values for selected radionu-

- clides and organs with the heart wall and heart contents as source organs. In *Proceedings of the Third International Symposium on Radiopharmaceutical Dosimetry*. Oak Ridge, Tennessee, October 7-10, 1980, Bureau of Radiological Health Report FDA 81-8166, 1981. (Supplemented by Coffey JL and Watson EE, unpublished data for S values for iron isotopes).
5. SNYDER WS, FORD MR, WARNER GG: Estimates of specific absorbed fractions for photon sources uniformly distributed in various organs of a heterogeneous phantom. *MIRD Pamphlet No. 5, Revised*. New York, Society of Nuclear Medicine, Jan 1978
  6. BROWNELL GL, ELLETT WH, REDDY AR: Absorbed fractions for photon dosimetry. *MIRD Pamphlet No. 3. J Nucl Med (Suppl 1) 9:27-39*, 1968
  7. ELLETT WH, HUMES RM: Absorbed fractions for small volumes containing photon-emitting radioactivity. *MIRD Pamphlet No. 8. J Nucl Med (Suppl 5) 12:25-32*, 1971
  8. SNYDER WS, FORD MR, WARNER GG, WATSON SB: A tabulation of dose equivalent per microcurie-day for source and target organs of an adult for various radionuclides. ORNL-5000, Oak Ridge National Laboratory, November 1974
  9. BAROSI G, BERZUINI C, CAZZOLA M, et al: An approach by means of mathematical models to the analysis of ferrokinetic data obtained by liquid scintillation counting of  $^{59}\text{Fe}$ . *J Nucl Biol Med* 20:8-22, 1976
  10. BOTHWELL TH, FINCH CA: Ferrokinetics. In *Iron Metabolism*. Boston, Little Brown & Co., 1962, pp 180-219
  11. CAVILL I, RICKETTS C: The kinetics of iron metabolism. In *Iron in Biochemistry*, Jacobs A, Worwood M, Eds. New York, Academic Press, 1974, pp 613-647
  12. CHANG LL: Tissue storage iron in Singapore. *Am J Clin Nutr* 26:952-957, 1973
  13. FINCH CA, DEUBELBEISS K, COOK JD, et al: Ferrokinetics in man. *Medicine* 49:17-53, 1970
  14. POLLYCOVE M: Hemochromatosis. In *The Metabolic Basis of Inherited Disease*, Stanbury JB, Wyngaarden JB, Fredrickson DS, Eds. New York, McGraw Hill Book Co., 1978, pp 1127-1164
  15. POLLYCOVE M: Iron metabolism and kinetics. *Semin Hematol* 3:235-298, 1966
  16. POLLYCOVE M, TONO M: Studies of the erythron. *Semin Nucl Med* 5:11-61, 1975
  17. SAITO H, YAMADA H: Studies on red cell production and destruction in various hematological disorders in view of ferrokinetics. *Acta Haem Jap* 36:681-709, 1973
  18. FAIRBANKS V, FAHEY JL, BEUTLER E: *Clinical Disorders of Iron Metabolism*. New York, Grune & Stratton, 1971
  19. PETTIT JE, LEWIS SM, WILLIAMS ED, et al: Quantitative studies of splenic erythropoiesis in polycythaemia vera and myelofibrosis. *Br J Haematology* 34:465-475, 1976
  20. HARRIS JW, KELLERMEYER RW: *The Red Cell*. Cambridge, Mass., Harvard University Press, 1970, pp 519-524
  21. COOK JD, PALMER HE, PAILTHORP KG, et al: The measurement of iron absorption by whole body counting. *Phys Med Biol* 15:467-473, 1970
  22. MCKEE LC, JR, PRICE R, JOHNSTON RE, et al: Long term studies of iron metabolism in normal males: Comparison of red blood cell radioactivity with whole-body counter data. *J Nucl Med* 15:156-160, 1974
  23. SARGENT T, POLLYCOVE M, CARPE L, et al: Dynamics of total body iron: Gastrointestinal, blood, storage and "fixed" components. *Clin Res* 10:78, 1962
  24. BERMAN M: Compartmental analysis in kinetics. In *Computers in Biomedical Research*. Stacy RW, Waxman BD, Eds. New York, Academic Press, 1965, Vol II, pp 173-201
  25. BRILL AB, PRICE RR: Iron metabolism and dosimetry in abnormals. In *Radioisotope Studies Utilizing a Low Level Whole Body Counter*. Oak Ridge National Laboratory Report ORO-2401-60, 1973, pp 7-14
  26. PRICE RR, MCKEE LC, JR, KRANTZ SB, et al: Estimation of slow dynamic function parameters in iron kinetics studies using quantitative measurements and compartmental modelling analysis. In *Dynamic Studies with Radioisotopes in Medicine*, 1974. Vienna, IAEA, 1975, Vol. 1, pp 429-444
  27. PRICE RR, JOHNSTON RE, BRILL AB, et al: Estimation of radioactive content of body organs by combining direct measurements and distribution models. In *Assessment of Radioactive Contamination in Man*. Vienna, IAEA, 1973, pp 47-57
  28. COFFEY JL, CRISTY M, WARNER GG: Specific absorbed fractions for photon sources uniformly distributed in the heart chambers and heart wall of a heterogeneous phantom. *MIRD Pamphlet No. 13. J Nucl Med* 22:65-71, 1981
  29. CLOUTIER RJ, WATSON EE: Radiation dose from radioisotopes in the blood. In *Medical Radionuclides: Radiation Dose and Effects*. Cloutier RJ, Edwards CL, Snyder WS, Eds. CONF-691212, Oak Ridge, TN, 1970, pp 325-345
  30. SNYDER WS, Chairman, *Report of the Task Group on Reference Man*, ICRP 23, New York, Pergamon Press, 1975
  31. GLASS HI, DE GARRETTA AC, LEWIS SM, et al: Measurement of splenic red-blood-cell mass with radioactive carbon monoxide. *Lancet* 1:669-670, 1968
  32. HEGDE UM, WILLIAMS ED, LEWIS SM, et al: Measurement of splenic red cell volume and visualization of the spleen with  $^{99m}\text{Tc}$ . *J Nucl Med* 14:769-771, 1973
  33. FERRANT A, CAUWE F: Quantitative organ-uptake measurement with a gamma camera. *European J Nucl Med* 4: 223-239, 1979
  34. BATEMAN S, LEWIS SM, NICHOLAS A, et al: Splenic red cell pooling: A diagnostic feature in polycythaemia. *Br J Haematol* 40:389-396, 1978
  35. FRANCOIS PE, SZUR L: Use of iron-52 as a radioactive tracer. *Nature* 182:1665-1667, 1958
  36. VAN DYKE D, ANGER H, POLLYCOVE M: The effect of erythropoietic stimulation on marrow distribution in man, rabbit, and rat as shown by  $\text{Fe}^{59}$  and  $\text{Fe}^{52}$ . *Blood* 24:356-371, 1964
  37. ANGER HO, VAN DYKE DC: Human bone marrow distribution shown in vivo by iron-52 and the positron scintillation camera. *Science* 144:1587-1589, 1964
  38. COTZIAS GC: Manganese in health and disease. *Physiol Revs* 38:503-532, 1958
  39. ATKINS HL, SOM P, FAIRCHILD RG, et al: Myocardial positron tomography with manganese-52m. *Radiology* 133:769-774, 1979
  40. HALPERN SE, HAGAN P, STERN P, et al: The effect of certain variables on the tumor and tissue distribution of tracers. III. Salicylates and vasoactive drugs. *Invest Radiol* 16:120-125, 1981
  41. National Council on Radiation Protection and Measurement: A Handbook of Radioactivity Measurements Procedures. Washington, D.C., NCRP Report No. 58, Nov 1, 1978
  42. HOUTERMANS H, MILOSEVIC O, and REICHEL F: Half-lives of 35 radionuclides. *Int J Appl Rad and Isotopes* 31: 153-154, 1980
  43. DILLMAN LT, VON DER LAGE FC: Radionuclide decay schemes and nuclear parameters for use in radiation-dose estimation. *MIRD Pamphlet No. 10*. New York, Society of Nuclear Medicine, Sept 1975
  44. LEDERER CM, SHIRLEY VS, Eds. Table of isotopes, Seventh Edition. New York, Wiley, 1978